Analysis of Nonlinear Wave Parameters on Ofir Sandy Beach (NW Portugal)

Tiago Abreu, Paulo A. Silva, Paulo Baptista, Joaquim Pais-Barbosa, Sandra Fernández-Fernández, Caroline Ferreira, and João Matos

Abstract

The characterization of wave transformation processes in the nearshore is of paramount importance when it comes to assessing storm and flooding impacts, sediment transportation and deposition, harbors safety or design of coastal protective structures. This study analyzes nonlinear wave parameters on Ofir sandy beach. This beach is located along the northwest Portuguese coast which is a highly energetic coast exposed to waves generated far away in the Atlantic Ocean. Despite the existence of rocky outcrops in the nearshore and intertidal zones at the study site, reducing the wave energy that reaches the beach, the study site exhibits pronounced erosive processes. Field observations of six near-bottom pressure records collected at the intertidal zone help to characterize the evolution of wave nonlinearities which are directly associated with sediment transport mechanisms. Data results show that there is an interrelation between the characteristics of the waves and the local morphology. It is also possible to ascertain, more clearly, the level of asymmetry present in the waves propagated at different depths, contributing to a better understanding of the local morpho-hydrodynamics.

Keywords

Nonlinear waves • Sandy beach • Relative wave height • Skewness • Asymmetry

1 Introduction

It is recognized that an accurate description of the wave phenomena and the wave governing mechanisms are of paramount importance for a good understanding of the morphodynamics of the coastal zone. In particular, within the context of coastal erosion, there is the need to collect data with sufficiently long records to establish wave conditions for engineering purposes. This kind of monitoring helps to improve our knowledge of sediment transport and it is obviously a good contribution to an integrated coastal management strategy (e.g., Ferreira and Matias, 2013).

The highly energetic northwest coast of Portugal faces severe erosion and Ofir is one of the example areas under threat, facing serious problems (Lira et al. 2016). Despite the existence of rocky outcrops in the nearshore and intertidal zones, that reduce the wave energy reaching the beach, the study site exhibits pronounced erosive processes.

This study analyzes nonlinear wave parameters on Ofir sandy beach based on a field survey data, where local hydrodynamic conditions and beach topography were recorded. Local wave gauge measures of the sea surface were obtained through bottom-mounted pressure sensors. In total, six near-bottom pressure transducers were deployed at different depths, collecting data at the intertidal zone. The instruments help to characterize the evolution of nonlinearities associated with nearshore wave transformations, which is intrinsically correlated with sediment transport mechanisms (e.g., Sancho et al. 2011).

T. Abreu (✉)
Civil Engineering Department, School of Engineering (ISEP), Polytechnic of Porto, Porto, Portugal
e-mail: taa@isep.ipp.pt

T. Abreu · P. A. Silva · P. Baptista · J. Pais-Barbosa · S. Fernández-Fernández · C. Ferreira
CESAM-Centre for Environment and Marine Studies, University of Aveiro, Aveiro, Portugal

P. A. Silva · S. Fernández-Fernández · C. Ferreira
Department of Physics, University of Aveiro, Aveiro, Portugal

J. Pais-Barbosa
Universidade Lusófona do Porto, Porto, Portugal

P. Baptista
Department of Geosciences, University of Aveiro, Aveiro, Portugal

J. Matos
Department of Mathematics, School of Engineering (ISEP), Polytechnic of Porto, Porto, Portugal

F. Fernandes et al. (eds.), *Advances in Natural Hazards and Hydrological Risks: Meeting the Challenge*, Advances in Science, Technology & Innovation,
https://doi.org/10.1007/978-3-030-34397-2_29

2 Study Site

2.1 Ofir Beach

Ofir beach is located between Cávado river mouth (Esposende city), at north, and Apúlia beach, at south (Fig. 1). The area is composed by palaeozoic schists and quartzite outcrops with an approximately NW-SE orientation. The nearshore area is clearly influenced by these outcrops due to a large stand between 5 and 10 m isobaths. Furthermore, at Ofir beach, the isobath of 5 m is 800 m far away of shoreline. Predominant waves come from WNW to NNW and have a mean significant wave height of 1.5–2.5 m and a peak period of 8–11 s. The existence of rocky outcrops in large areas of the nearshore and intertidal zone at the study site influences the wave characteristics, reducing the wave energy reaching the beach. The tidal regime is semidiurnal. Beach sediments are composed by medium sand (d_{50} = 0.34 mm) with significant amount of mafic minerals representative of the rocky outcrops (Fernández-Fernández et al. 2016).

2.2 Field Survey

The field survey was conducted on October 4th, 2013, during a complete tidal cycle from 9 h 06 min to 21 h 29 min (local time) with a tidal range of 2.85 m. Two shore-normal arrays of pressure transducers (PT—Level TROLL 500 In Situ) were installed at approximately 0.10 m above the sand bed at the intertidal zone and small changes of around 0.02 m were observed at the end of the tidal cycle. The PT was attached to metallic structures and recorded near-bottom pressure time-series with a sampling frequency of 2 Hz. The PT horizontal positions (cross-shore coordinate x) and the vertical coordinate z referred to the high tide level as $z = 0$ are shown in Fig. 2. Both PT1 and PT4 were installed at the seaward-most locations and although in different shore-normal arrays, they practically possess the same cross-shore position.

The offshore wave conditions (significant wave height, H_s, wave peak period, T_p, and direction) were recorded at the Leixões wave buoy. This buoy is located approximately 28 km SW from the study site, at a depth of 83 m

Fig. 1 Study area

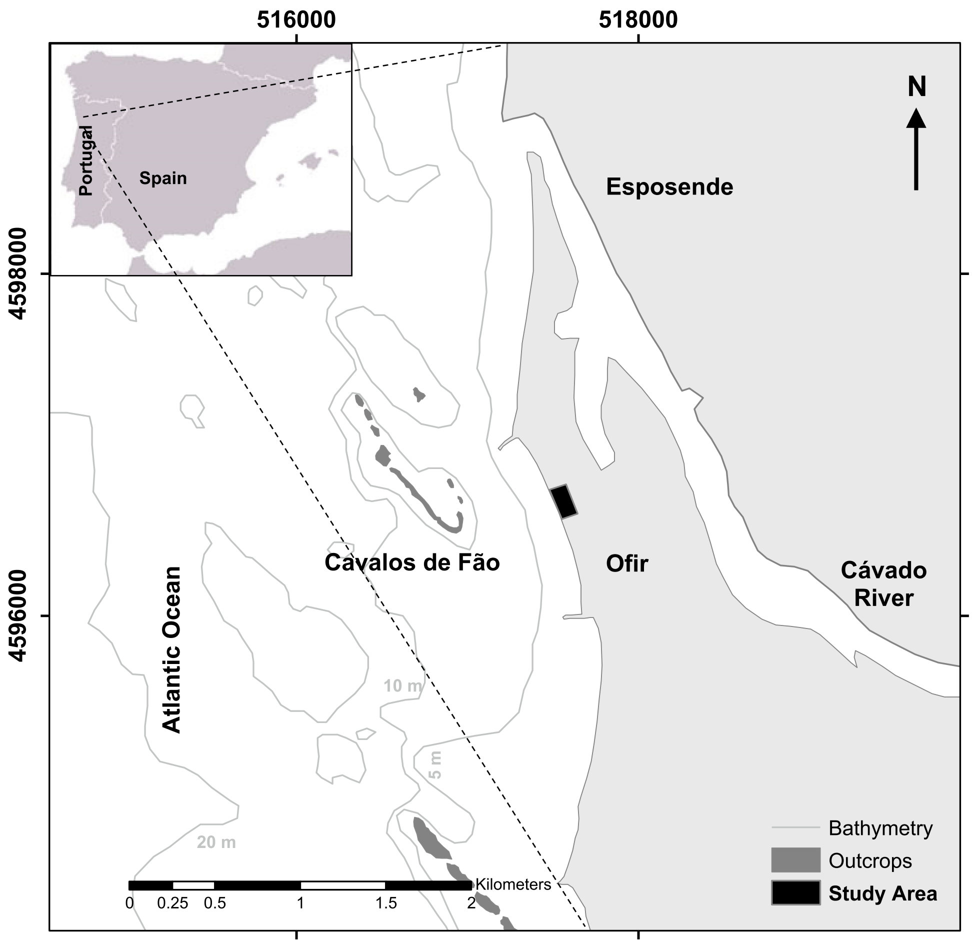

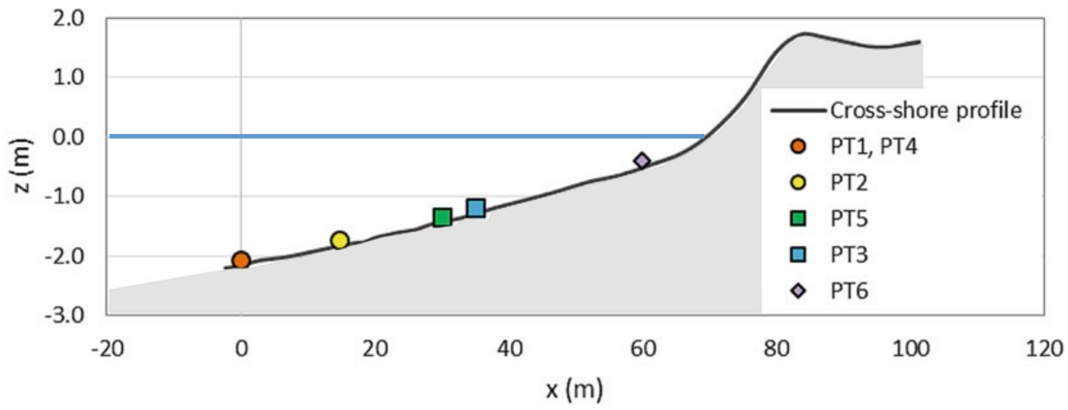

Fig. 2 Ofir beach cross-shore profile and pressure transducer (PT) locations

(41.31 N, 8.95 W) and is operated by the Portuguese Hydrographic Institute (IH). The offshore wave climate showed incident waves from NW, with a mean value of H_i of 1.5 m, during the survey period and an average T_p of 8.0 s.

The INSHORE (INtegrated System for High Operational REsolution in shore monitoring) system was used to obtain the topography of the beach (Baptista et al. 2011). Two surveys of the site were made, at both low tides of that day.

3 Results

All the information gathered with the PT when they were immersed, in the shoaling and surf zones, was used to characterize the wave data at the beach during this tidal cycle. The pressure data measured with the PT were corrected taking into account the atmospheric pressure values measured when the sensor was dry (at low tide). To compute the water depth, the distances of the sensor to the bed were also taken into account. Because of the attenuation of wave-induced pressure fluctuations with increasing depth and frequency, a pressure response correction was considered to compute the sea surface elevation.

The water depth at each instant was computed from the measured PT sea surface water level, by applying a Butterworth low-pass filter with a cut-off frequency of 0.05 Hz. The remaining signal at high frequencies consists of short gravity waves. Both records were divided into 20-min intervals from which the mean water depth, h, and both H_s and T_p were computed. The data corroborates the offshore T_p of 8.0 s but the mean H_s value at high tide is 0.8 m, falling to about half of the offshore value ($H_s \approx 1.5$ m). This difference reveals a strong attenuation of wave energy, which is expected to occur in Ofir Beach as a consequence of the natural outcrops (e.g., Fernández-Fernández et al. Silva 2016).

Figure 3 shows the water depth obtained for each pressure transducer (PT) and the corresponding significant wave height to water depth ratio ($\gamma = H_s/h$). As can be seen in Fig. 3a, the landward-most PT (PT6) was located above the other devices and recorded mainly data in the swash zone. Therefore, it was cut-off from the PT records and it is not considered in the present analysis. For the other PT, the comparison of both panels in Fig. 3, allows to estimate at which time the data should not be considered in the analysis. For example, the peak values of water depth ratio for PT1 or PT2 (see Fig. 3b) indicate that the shoaling and surf zone periods is between 11 h 25 min and 19 h 31 min. Immediately before or after, the devices are in the swash zone or the tide level did not reach the instruments.

The relative wave height γ presented in Fig. 3b is one of the most important parameters in the nearshore. Indeed, most of the computational models rely on linear wave theory, aiming to predict surf zone hydrodynamics. Inside the surf zone, one expects a decrease in wave height, to a point where it can be described as a linear function of the local depth (e.g., Poate et al. 2018). Upper bound values of γ were extensively studied, both at breaking (the so-called breaker index γ_b) and non-breaking waves (γ) and its limits are of obvious significance for engineering purposes. The central part of Fig. 3b, corresponding to the high tide, shows that the values of γ increase for decreasing depths from about 0.38 (PT1) to 0.68 (PT3). Similar reasoning can be observed along time when the highest γ values are due to broken waves that start to reach the devices and its values reduce when the water depth increases. This is consonant with breaking characteristics since the wave propagation phenomenon exerts its influence on the relative wave heights γ inside the surf zone (Masselink, 1993).

Figure 4 shows two other parameters calculated from the acquired sea surface elevation, η, that measure the wave shape transformation as waves shoal and break into the nearshore for PT1 and PT4. These parameters are the

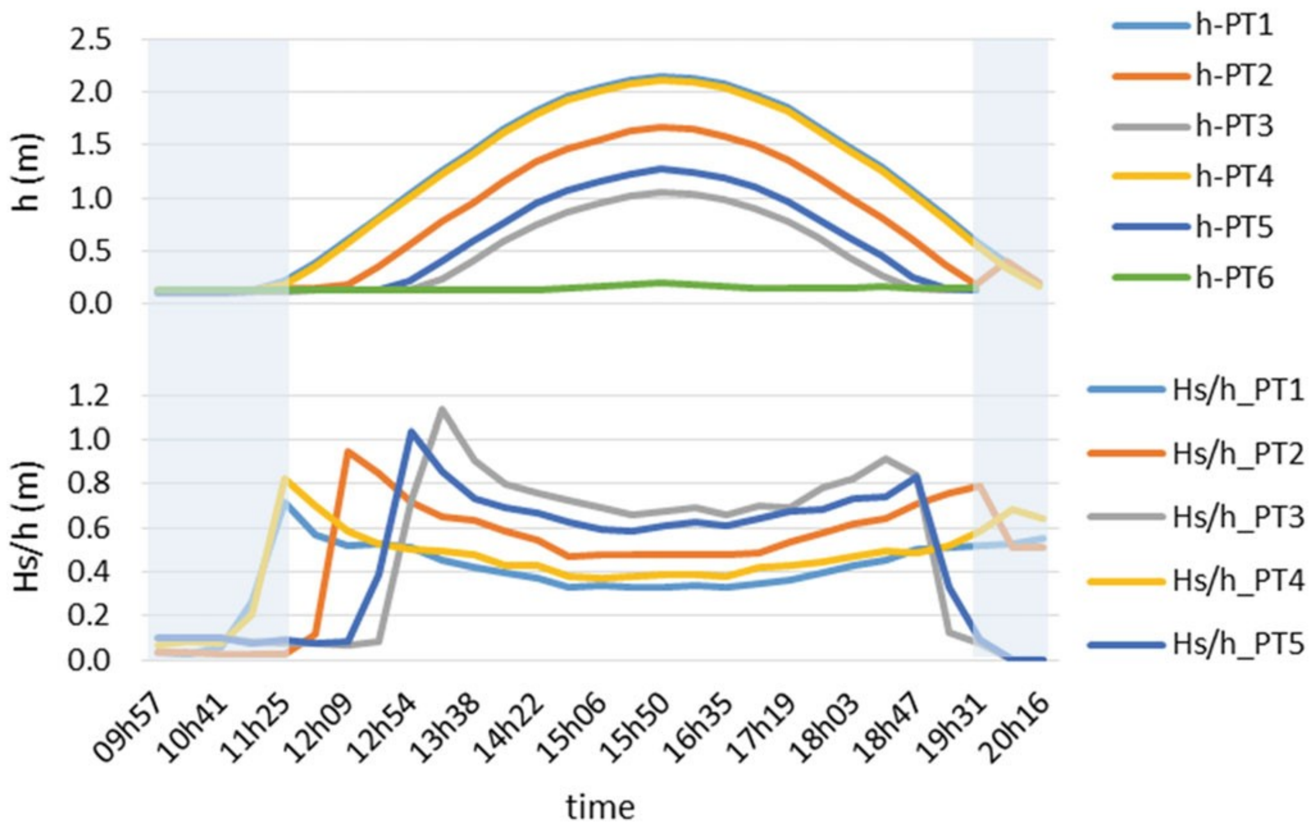

Fig. 3 **a** Depth obtained for each pressure transducer (PT) location and **b** corresponding significant wave height to water depth ratio

skewness coefficient ($R = \eta_{max}/(\eta_{max} - \eta_{min})$) and the "acceleration skewness parameter" ($\alpha = 2T_{pc}/T$), where T is the wave period η_{max} and η_{min} are the η values at the crest and wave trough, respectively, and T_{pc} is the time interval measured from the zero up-cross point to η_{max}. Respectively, these parameters are linked with the so-called skewness *Sk* (which is a measure of horizontal wave shape mutation, i.e., crest-trough differences in a wave) and asymmetry *As* (which is a measure of vertical wave shape transformation, i.e., left-right differences in a wave).

Looking to the variation of R and α for PT1 and PT4, a better insight on the phenomena can be provided. For symmetric oscillatory motions, R equals 0.5, whereas when the magnitude of velocity at the crest is larger than that at the trough one obtains $R > 0.5$. It is clearly seen that the value of R increases with depth reduction, h.

The values of α are also different than 0.5, which is the representative value of a linear (sinusoidal) motion. The observed differences mean that the depth reduction is associated with nonlinear transformations, the wave is pitching forward (sawtooth shape) and the acceleration skewness is playing an important role in sediment transport (Sancho et al. 2011).

4 Concluding Remarks

This study analyzes nonlinear wave parameters on Ofir sandy beach, assessing systematic changes in the wave shape as they shoal and break into the nearshore. The data was collected during a complete tidal cycle at the intertidal zone during a field survey, using six near-bottom pressure transducers. The instruments help to characterize the evolution of nonlinearities associated with nearshore wave transformations, which is intrinsically correlated with sediment transport mechanisms.

The analysis of the relative wave height discloses that its values increase for decreasing depths, revealing an interrelation between the characteristics of the waves and the local morphology. It is also possible to ascertain, more clearly, the

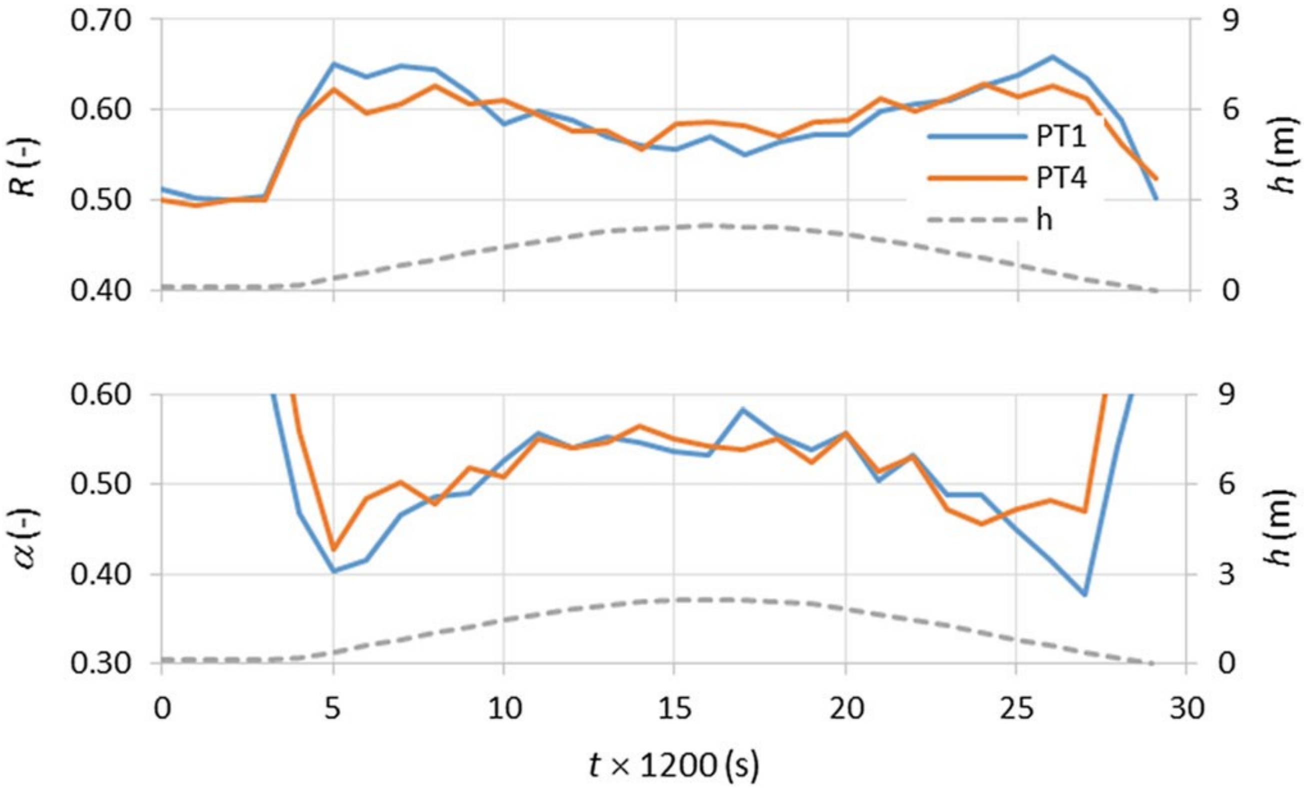

Fig. 4 **a** Skewness coefficient for PT1 and PT4 and **b** "acceleration skewness parameter" for PT1 and PT4

level of skewness and asymmetry present in the waves propagated at different depths, contributing to a better understanding of the local morpho-hydrodynamics. The results are analyzed for the complete tidal cycle highlighting an increase of the nonlinearities with the reduction of depth.

Acknowledgements Thanks are due to the financial support to CESAM (UID/AMB/50017/2019), to FCT/MEC through national funds, and the co-funding by the FEDER, within the PT2020 Partnership Agreement and Compete 2020. This work is a contribution to project SANDTRACK (POCI-01-0145-FEDER-031779) funded by FEDER, through COMPETE2020 - Programa Operacional Competitividade e Internacionalização (POCI), and by national funds (OE), through FCT/MCTES.

References

Baptista P, Cunha T, Bernardes C (2011) The validation analysis of the INSHORE system: a precise and efficient coastal survey system. Environ Monit Assess 179(1–4):589–604

Fernández-Fernández S, Baptista P, Martins V, Silva, PA, Abreu T, Pais-Barbosa J, Bernardes C, Miranda P, Rocha M, Santos F, Bernabeu A, Rey D (2016) Longshore transport estimation on Ofir beach (NW Portugal): sand tracers experiment. J Waterw Port Coast Ocean Eng 142(2), 04015017:1-14

Ferreira O, Matias A (2013) Coastal erosion and protection in Europe, 1st edn. Pranzini E, Williams A, London

Lira CP, Silva AN, Taborda R, Andrade CF (2016) Coastline evolution of Portuguese low-lying sandy coast in the last 50 years: an integrated approach. Earth Syst Sci Data 8:265–278

Masselink G (1993) Attenuation coefficients on natural beaches. In: 11th Australasian conference on coastal and ocean engineering, 105–111

Poate T, Masselink G, Austin MJ, Dickson M, McCall R (2018) The role of bed roughness in wave transformation across sloping rock shore platforms. J Geophys Res Earth Surf 123(1):97–123

Sancho F, Abreu T, D'Alessandro F, Tomasicchio GR, Silva PA (2011) Surf hydrodynamics in front of collapsing coastal dunes. J Coast Res SI 64(1):144–148